Evaluation of the mechanical efficiency of knee braces based on computational modelling

Baptiste Pierrat, Jérôme Molimard, Laurent Navarro, Stéphane Avril, Paul Calmels

Computer Methods in Biomechanics and Biomedical Engineering
Vol. 00, No. 00, Month 200x, 1–22

RESEARCH ARTICLE

Evaluation of the mechanical efficiency of knee braces based on computational modelling.

Baptiste Pierrat[a,b,*], Jérôme Molimard[a], Laurent Navarro[a], Stéphane Avril[a], Paul Calmels[c]

[a] *Ecole Nationale Supérieure des Mines, CIS-EMSE, CNRS:UMR5307, LGF, F-42023 Saint-Etienne, France*
[b] *Pôle des Technologies Médicales, F-42000 Saint-Etienne, France*
[c] *Laboratoire de Physiologie de l'Exercice (LPE EA 4338), Université de Saint-Etienne, F-42055 Saint-Etienne, France*

(*Received 00 Month 200x; final version received 00 Month 200x*)

Knee orthotic devices are commonly prescribed by physicians and medical practitioners for preventive or therapeutic purposes on account of their claimed effect: joint stabilization and proprioceptive input. However, the force transfer mechanisms of these devices and their level of action remains controversial. The objectives of this work are to characterize the mechanical performance of conventional knee braces regarding their anti-drawer effect using a Finite Element Model of a braced lower limb. A design of experiment approach was used to quantify meaningful mechanical parameters related to the efficiency and discomfort tolerance of braces. Results show that the best tradeoff between efficiency and discomfort tolerance is obtained by adjusting the brace length or the strap tightening. Thanks to this computational analysis, novel brace designs can be evaluated for an optimal mechanical efficiency and a better compliance of the patient with the treatment.

Keywords: knee braces; knee orthoses; efficiency; discomfort tolerance; finite element

1. Introduction

The knee is the largest joint in the body and supports high loads, up to several times the body weight. It is vulnerable to injury during sport activities and to degenerative conditions such as arthrosis. Various syndromes are associated with an increased knee laxity, leading to a functional instability (*i.e.* a 'wobbly' feeling). The anterior cruciate ligament (ACL) is the main postero-anterior (P-A) stabilizing structure, preventing the knee from an anterior drawer movement, for instance when walking upstairs (Vergis et al. 1997). The ACL is involved in 24% of all knee injuries and 59% of ligamentous injuries (Bollen 2000). In the United States,the annual incidence in the general population is approximately 1 in 3500 with 100,000 ACL reconstructions performed each year (Gordon and Steiner 2004; Miyasaka et al. 1991). These conditions are a huge burden on individuals and healthcare systems.

Knee braces or orthoses are commonly prescribed by physicians and medical practitioners for pathologies involving knee pain/laxity. This choice is related to their claimed mechanical effects but rely on very few assessments, from biomechanical

*Corresponding author. Email: baptiste.pierrat@gmail.com

ISSN: 1741-5977 print/ISSN 1741-5985 online

DOI: 10.1080/1741597YYxxxxxxxx
http://www.informaworld.com

studies to therapeutic trials (Thoumie et al. 2001, 2002). Numerous action mechanisms have been proposed and investigated such as: proprioceptive improvements (Barrack et al. 1989; Corrigan et al. 1992; McNair et al. 1996; Birmingham et al. 2001; Thijs et al. 2009), strain decrease on ligaments (Beynnon et al. 1997; Beynnon and Fleming 1998; Fleming et al. 2000; Hinterwimmer et al. 2004), neuromuscular control enhancement (Osternig and Robertson 1993; Ramsey et al. 2003; Théoret and Lamontagne 2006) and joint stiffness increase (Lunsford et al. 1990). Other studies aimed to justify the use of knee orthoses in medical practice. These studies were reviewed by Paluska and McKeag (2000); Thoumie et al. (2001, 2002); Genty and Jardin (2004); Beaudreuil et al. (2009). The following conclusions can be drawn from the literature:

(1) Mechanical/physiological effects have been emphasized, but these mechanisms have been poorly characterized.
(2) Only a few high-level clinical studies exist, and the effectiveness of bracing versus no bracing on improving joint stability or reducing pain has not been conclusively demonstrated in practice.

Possible explanations of (1) having no perceptible effect on (2) are that mechanical action levels are too low, or that patients do not comply to the orthopedic treatment and do not wear enough the device due to comfort issues. What is more, subjective evaluations of patients highlight a large demand for these products; therefore, their efficiency is still widely discussed among medical experts.

As a consequence of these uncertainties, medical practitioners and manufacturers still lack a simple evaluation tool for knee orthoses. A French committee of experts highlighted this problem (Ribinik et al. 2010) and stated that orthoses must be evaluated by taking both the mechanisms of action and the desired therapeutic effects into account. Mechanical actions of knee orthoses have been evaluated using experimental devices either on cadaveric knees (France and Paulos 1990) or on surrogate limbs (Paulos et al. 1987; France et al. 1987; Cawley et al. 1989; Lunsford et al. 1990). However, the cadaveric knee method leads to unreliable results because of substantial scatter (anatomical, physiological and methodological variances); as for the surrogate method, phantoms consisted in mechanical parts mimicking the joint, thigh and leg on which a specific kinematics was simulated (drawer, pivot shift, lateral impact...), and instrumented with tensiometers in order to quantify the mechanical effects of a brace. These devices were poorly representative of a real human limb (skin and soft tissue behaviour). What is more, tests were conducted on very specific braces and do not allow to understand bracing mechanisms in general. Besides, these tests are far from accurate in reproducing the dynamical conditions of real movements (running, walking...). Finite Element (FE) analysis is a powerful tool when it comes to complex mechanical simulations and would definitely help to understand force transfer mechanisms and unveil the influence of different brace characteristics. To our knowledge, there is no published computational analysis of a brace/limb system, although it would answer most of the above concerns.

An original FE model approach has been developed and is presented in this paper. This model was built in agreement and cooperation with medical practitioners and orthotic manufacturers, in a tentative of linking design problems, brace ability to prevent a given pathology (ACL deficiency) and brace discomfort tolerance. Studies dealing with passive motion of the knee using Robotic Testing Systems (Woo et al. 1998; Lujan et al. 2007) reported that removing the ACL greatly increases anterior tibial translation and reduces internal tibia rotation under an anterior load; knee braces prescribed for this condition should compensate this laxity and stiffen the joint in this direction. An efficiency evaluation index reflecting this objective is

Figure 1. Usual mass-produced knee brace with product characteristics.

needed.

As there is a huge variety of orthoses on the market, the focus was placed on manufactured knee braces, in opposition to individualized, custom-made orthotic devices. They are usually made of synthetic fabrics and may incorporate bilateral hinges and bars, straps, silicone anti-slipping pads and patella hole. A typical design of an usual brace is depicted in Figure 1. Such braces are prescribed either for prophylactic or functional purposes (Thoumie et al. 2001).

This paper is organized as follows. First, we will present the development of the FE model of a braced knee including the geometry, mesh, constitutive parameters and boundary conditions (BCs). Then we will explain how this tool has been used to assess the brace effectiveness against a drawer movement, using a design of experiment approach in order to account for various brace designs. Finally we will propose an optimization criterion to maximize the brace effectiveness while limiting discomfort tolerance issues.

2. Methods

2.1 Finite element model of the braced knee

The model was developed under Abaqus® v6.10-2. It was built as a generic tool to understand the force transfer mechanisms between the rigid parts of the knee brace (hinged bars) and the joint (bones). The aim was to investigate how this force transfer is altered by the deformation of the brace fabric and the patient soft tissues on the one hand, and sliding phenomena at the interfaces on the other. To this end, some geometrical and mechanical parameters were considered as factors and their influence on the global response were characterized.

2.1.1 The deformable limb

2.1.1.1 Geometry. 3D geometry of the human lower limb was obtained from a whole body PET-CT (Positron Emission Tomography - Computed Tomography) scan. This scan comes from an online DICOM sample image sets (Melanix 2012). The DICOM data states that the subject is a 34 year old female. The lower body consisted of about 500 slices of thickness 2 mm, and size 512x512 pixels with 0.98 mm/pixel resolution. A limb was cropped and segmented using the software

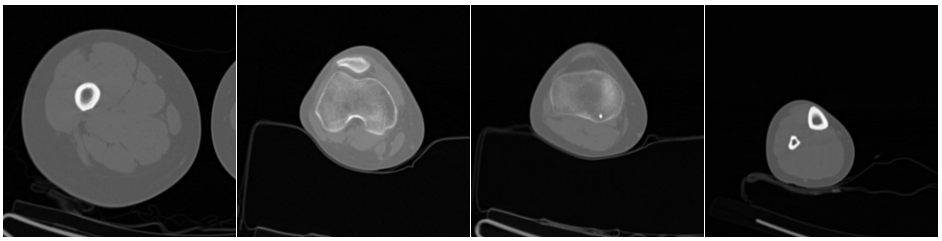

(a) Pet-CT scan slices from the thigh to the leg (left-right).

(b) Corresponding images after segmentation.

Figure 2. Illustration of the segmentation process.

ImageJ (Rasband 2011). Segmentation was performed by thresholding, resulting in one material identified as soft tissues after removal of bones areas and skin, as depicted in Figure 2.

A fine 3D mesh of the segmented stack was imported in Rhinoceros® v4.0 for surface reconstruction. Finally, surfaces were imported in Abaqus® in order to control mesh generation from this software. Skin was generated by offsetting the external boundary of the soft tissue part, resulting in a separate layer of thickness 1 mm (Evans and Holt 2009). The thigh was separated from the leg in order to get two separate parts as seen in Figure 3. This last step was done in order to avoid any internal knee stiffness and in a concern of modelling knee kinematics without convergence problems due to the high deformation of elements in the centre knee area. Patella was modelled as a separate shell part. Finally, the limb was scaled in order to reach the dimensions of a median French male limb (Institut Français du Textile et de l'Habillement 2006): circumference at the knee: 38 cm; +15 cm above the knee: 49.3 cm; -15 cm below the knee: 36.2 cm. The resulting parts can be seen in the exploded view of the assembly in Figure 3. It is noteworthy that the limb is not fully extended, it is slightly bent with an angle of 20°.

2.1.1.2 Mesh. Soft tissues of the thigh and leg were respectively meshed with 37572 and 22627 reduced linear hexahedral elements of type C3D8R (Abaqus 2010) using a custom meshing algorithm written in Python® allowing a finer mesh at the skin interface and a coarser mesh around the bones. During this step the bone geometry was simplified. The patella was meshed with shell elements: 714 reduced linear quadrilateral elements of type S4R and 26 reduced linear triangular elements of type S3R (Abaqus 2010). The skin was meshed with 22648 linear hexahedral elements of type C3D8 (Abaqus 2010) using an offset algorithm, with two elements in the thickness. The resulting meshes are depicted in Figure 3.

2.1.1.3 Materials. The soft tissue material was defined as homogeneous, isotropic, quasi-incompressible and hyper-elastic. A Neo-Hookean strain energy function was used (Linder-Ganz et al. 2007; Avril et al. 2010; Dubuis et al. 2012).

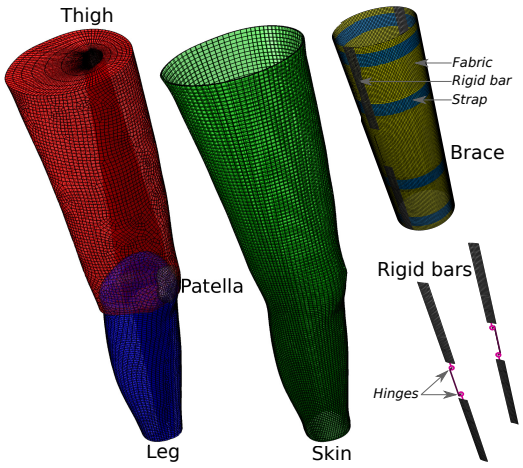

Figure 3. Exploded view of the different meshed parts constituting the deformable limb (thigh, leg, patella, skin layer) and the brace with a detail on the hinged rigid bars only.

This function may be written:

$$W = \frac{G}{2}(\overline{I_1} - 3) + \frac{K}{2}(J-1)^2 \tag{1}$$

where G and K are the material parameters, $\overline{I_1} = Tr(\overline{\mathbf{F}}.\overline{\mathbf{F}}^t)$ is the first deviatoric strain invariant, $J = det(\mathbf{F})$ the volume ratio, $\mathbf{F}$ the deformation gradient, $\overline{\mathbf{F}} = J^{-1/3}\mathbf{F}$ the deviatoric part of the deformation gradient and Tr the trace of a matrix. The constitutive properties represent the homogenized properties of muscles, fat, tendons and fascias. Values for G have already been identified for the leg for both passive muscles (G = 5 kPa) by Dubuis et al. (2012) and contracted muscles (G = 400 kPa) by Iivarinen et al. (2011). Soft tissue stiffness was considered as a parameter in the model to account for passive/active muscles. K was set such as $K = 100G$ in order to have a quasi-incompressible material (corresponding to an initial Poisson's ratio of 0.49). Bones were modeled as rigid bodies by fixing the surface nodes. The skin material was defined as homogeneous, isotropic, quasi-incompressible and hyper-elastic. An Ogden strain energy function was used (Evans and Holt 2009; Flynn et al. 2010). This function may be written:

$$W = \frac{2\mu}{\alpha^2}(\overline{\lambda}_1^{\alpha} + \overline{\lambda}_2^{\alpha} + \overline{\lambda}_3^{\alpha}) + \frac{K}{2}(J-1)^2 \tag{2}$$

where α, μ and K are the constitutive parameters, $\overline{\lambda}_i = J^{-1/3}\lambda_i$ are the deviatoric principal stretches, λ_i the principal stretches, $J = det(\mathbf{F})$ the volume ratio and $\mathbf{F}$ the deformation gradient. Values of α and μ have been identified by Evans and Holt (2009) on the forearm. μ was set to 130 Pa, α to 26 and K to 6.5 kPa. Evans and Holt (2009) also identified an initial strain of 0.2, so a corresponding pre-stress of 1.35 kPa was applied in circumferential and longitudinal directions of the skin at the start of the analysis.

2.1.2 The orthosis

2.1.2.1 Geometry. Geometry of the orthosis was designed from determination of the mechanically important features of usual existing braces. The identified features, as depicted in Figure 1, are:

- three metal bars on each side.

- An articulated system between bars consisting of two hinges on each side with a blocking feature to prevent hyper-extension.
- A polymeric textile with identified orientations.
- Fitting straps made of a different, stiffer textile.

The orthosis was generated as a slightly conical cylinder. Different regions were defined on the part: brace fabric, rigid bars and straps (Figure 3), each of which was assigned different mechanical properties. Rigid bars were connected using hinge connectors (Abaqus 2010) with a blocking feature, allowing them to pivot with the joint but blocking them in hyper-extension. An assumption was made that a patella hole, which is a circular opening above the patella area, as seen in Figure 1, has not a significant mechanical effect on the brace stiffness, hence the choice not to model it. The resulting brace model is reported in Figure 3. The size (cylinder circumference) and length (cylinder height) of the brace were considered as parameters in the model.

2.1.2.2 Mesh. The orthosis was meshed with reduced linear quadrilateral shell elements of type S4R (Abaqus 2010). The number of elements varied from 14790 to 43690 depending on the length of the brace.

2.1.2.3 Material. Mechanical behaviour of fabric has been already successfully modelled using shell elements (Yu et al. 2000). The material was defined as homogeneous, orthotropic and linear elastic. The constitutive equations, written in vectorial form, are:

$$\begin{pmatrix} N_{11} \\ N_{22} \\ N_{12} \end{pmatrix} = \begin{pmatrix} \frac{E_1}{1-\nu_{12}\nu_{21}} & \frac{\nu_{21}E_1}{1-\nu_{12}\nu_{21}} & 0 \\ \frac{\nu_{12}E_2}{1-\nu_{12}\nu_{21}} & \frac{E_2}{1-\nu_{12}\nu_{21}} & 0 \\ 0 & 0 & G_{12} \end{pmatrix} \begin{pmatrix} \epsilon_{11} \\ \epsilon_{22} \\ 2\epsilon_{12} \end{pmatrix} \tag{3}$$

and

$$\begin{pmatrix} M_{11} \\ M_{22} \\ M_{12} \end{pmatrix} = \begin{pmatrix} F_1 & \mu_2 F_1 & 0 \\ \mu_1 F_2 & F_2 & 0 \\ 0 & 0 & \tau_{12} \end{pmatrix} \begin{pmatrix} \kappa_{11} \\ \kappa_{22} \\ 2\kappa_{12} \end{pmatrix} \tag{4}$$

where N_{ij} and M_{ij} are the tensions and bending moments of the fabric, ϵ_{ij} and κ_{ij} the strains and bending strains, E_i the tensile rigidities, G_{12} the shear rigidity, ν_{ij} the Poisson's ratios, F_i the bending rigidities, τ_{12} the torsional rigidity and μ_i parameters analogous to Poisson's ratios. Subscripts 1 and 2 represent the longitudinal and circumferential directions of the brace cylinder and the directions along and across the straps respectively.

Tensile rigidities, shear rigidity and Poisson's ratios were obtained from unidirectional and off-axis tensile tests on an Instron® machine at speeds of 50 mm/min on 40×20 mm fabric samples. The linear elasticity assumption was judged reasonable from tensile tests for strains $\leq$40%. Bending rigidities were measured using a KES-F (Kawabata Evaluation System for Fabrics) device (Yu et al. 2000; Wu et al. 2003). Samples were taken from four commercially available orthoses and their straps. Fabric stiffness was considered as a parameter in the model. In order to reduce the number of parameters and based on measured properties, only E_1 varied and the other properties were derived as reported in Table 1. The strap properties were consistent among braces and are provided in Table 1.

Table 1. Mechanical properties of brace and strap fabrics.

Property	$E_1 = E_2$ (N/m)	G_{12} (N/m)	$\nu_{12} = \nu_{21}$	$F_1 = F_2$ (N.m)	τ_{12} (N.m)	$\mu_1 = \mu_2$
Brace	$[5000; 20000]$	$E_1/3$	0	$f(E_1)^*$	$F_1/3$	0
Straps	26400	9100	0.45	10^{-3}	0.5×10^{-3}	0

$^* f(E_1) = 2.37 \times 10^{-4}\ log(E_1) - 1.415 \times 10^{-3}$ (from mechanical characterization)

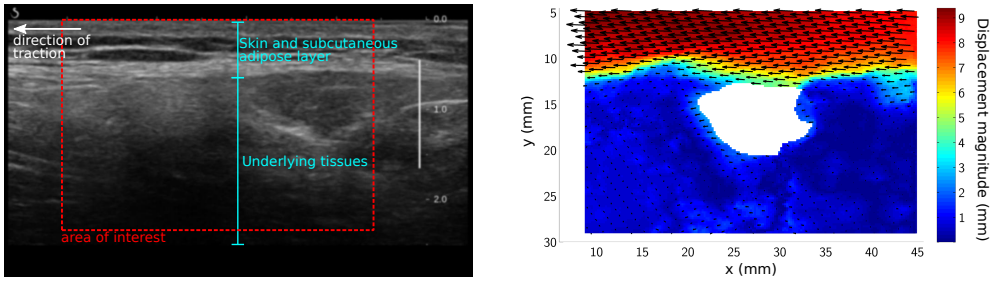

(a) Reference image. *(b)* Correlated displacement.

Figure 4. (a) Reference image in the sagittal plane as observed by ultrasound. Scale is in cm. (b) Correlated displacement in the area of interest after a 10 N pull of the skin. The white area correspond to a place where the correlation process failed. Scale of the arrows is 1/5.

The bars were modelled as rigid, considering the fact that they are usually made of 2 mm thick aluminium.

2.1.3 Interfaces

A basic Coulomb friction model was used for the orthosis/skin and skin/soft tissues interactions in which contact pressure is linearly related to the equivalent shear stress with a constant friction coefficient μ. Values of μ for different fabric/skin systems are available in the literature, averaging 0.7 for Spenco® (Sanders et al. 1998), or ranging from 0.3 (Teflon®) to 0.43 (cotton and polyester) (Gerhardt et al. 2009).

Concerning the skin/soft tissues contact, the choice of modelling skin as a separate layer comes from a preliminary study, in which the effect of in-plane pulling of the skin on an area 10 cm above the knee was observed by ultrasound (Aixplorer® system with auto time gain compensation mode). A 10 N traction was performed using duct tape and displacements of the skin and underlying structures were observed in the sagittal plane (4(a)). The PIV (Particle Image Velocimetry) ImageJ plugin (Rasband 2011; Tseng 2011) was used on 1166×666 pixels images with successive interrogation window sizes of 160×160;100×100;70×70 pixels to compute the displacement field (4(b)), showing a very narrow gliding plane between the skin/fat and underlying structures. From the work of Guimberteau et al. (2005), who described this interface, it is probable that modelling a separate layer is a good approximation of this mechanical behaviour, as long as slipping magnitudes are relatively small (∼1 cm in the case of these observations). No data was found in the literature for friction coefficient measurements of this interface, but a value of 0.1 was chosen from measurements of this coefficient between tendons and the structures over which they slide (Albin 1987). Skin was attached to soft tissues at the top and bottom of the limb.

No contact was defined between the thigh and leg.

2.1.4 Analysis steps and BCs

A quasi-static analysis was performed using the Explicit solver (Abaqus 2010) in order to solve significant discontinuities (fabric creases, contacts). Time scale and material density were carefully chosen to prevent dynamic effects (kinetic energy

Table 2. Selected model factors with their domains.

Factor name	Description	Domain
Soft tissue stiffness	Neo-Hookean parameter G for passive/contracted soft tissues of the limb, as described in Section 2.1.1.3	5|400 kPa *
Brace size	Brace cylinder circumference at the knee, as described in Section 2.1.2.1	28–38 cm **
Brace length	Brace cylinder height, as described in Section 2.1.2.1	17|34|51 cm *
Fabric stiffness	Single parameter to account for brace fabric stiffness, as described in Section 2.1.2.3	0.5–2 kN/m **
Brace/skin friction coefficient	Orthosis/skin Coulomb friction coefficient, as described in Section 2.1.3	0.1–1 **
Initial strap tightening	Initial strain along strap to account for strap tightening, as described in Section 2.1.4	5–15 % **

*Discrete factor.

**Continuous factor.

was much inferior to external work). The simulation consisted in three steps:

Step 1: a displacement field was applied to the brace to enlarge it and make it fit at the right place around the joint. The pre-stress was applied to the skin.

Step 2: contacts were activated, previously applied displacements were released in order to let the brace compress the limb and reach the mechanical equilibrium; bones were fixed; the straps were pre-stressed to simulate a real fitting (this pre-stress was considered as a parameter).

Step 3: a joint kinematics was imposed on the tibia/fibula, in this case a 1-DOF (Degree Of Freedom) P-A drawer of magnitude 20 mm; femur and patella were fixed.

2.2 Design of experiment approach

In order to study the influence of several mechanical and geometrical parameters of the brace/limb system, a design of experiment technique was used. It consists in selecting relevant parameters, choosing a plausible domain for each of them, using a sampling method to pick the different experimental points, run the analyses, choose one or several output data, extract the outputs from the analyses and build one or several response surfaces from these output data.

2.2.1 Parameter screening and domain selection

The basic ideas, terminology and techniques of design of experiments was explained by Goupy and Creighton (2007). Six parameters, or factors, were selected. Definition of these factors and the selected domains are reported in Table 2.

Soft tissue stiffness was used as a 2-level factor to reproduce the passive/contracted stiffness of the limb. As a consequence, it involves the following approximations: the contracted limb has the same geometry than the passive limb and the stiffness increase is homogeneous and isotropic. This factor is preponderant compared to inter-individual stiffness variability as there is a factor 80 between passive and active muscles. The brace circumference domain is justified as the indicated brace size for the limb (manufacturer's size table) $\pm$ 1 size. Brace length is usually consistent between brace manufacturers but no scientific argument supports this choice. It corresponds to the intermediate value of our 3-level factor (34 cm). The lower level is supposed to be the minimum length to tighten the straps above and below the joint (17 cm), and the upper level is 51 cm. Fabric stiffness was slightly extrapolated from mechanical characterization: usual braces are made with fabrics of stiffness usually comprised between 0.5 and 1.5 kN/m.

The orthosis/skin friction coefficient ranged from 0.1 to 1 (see Section 2.1.3). This factor domain would need to be supported by tribological characterization of different fabric/skin interfaces with and without anti-sliding features. Finally, initial strap tightening ranged between 5 and 10 %. The lower value of its domain is just enough to contact the skin without applying a significant pressure while the higher value roughly corresponds to highly tightened straps on a subject with a similar brace.

2.2.2 Sampling method

The use of Latin hypercube for efficient sampling has been described by Olsson et al. (2003). This sampling method corresponds to the generalization of Latin squares in multiple dimensions. It allows variance reduction by partitioning the input factor space into equal probability disjoint sets. This method was first introduced in 1979 by McKay et al. (1979). It was chosen in a concern of finding a good balance between total computational time and study domain coverage. The principle of Latin hypercubes is to partition a space of n factors into m^n parts, each factor being divided into m equally probable intervals. Then, m samples are taken in the n dimensions space so that only one division of each factor contains one sample. Stratified Latin hypercube is a special type of Latin hypercube in which discrete factors are allowed (Matlab 2011). The choice of the stratified Latin hypercube was done because two of the six factors are discrete. Variables were centred around 0 and scaled to a $[-1; 1]$ interval, resulting in coded variables. There are several methods used to construct the Latin hypercube, we chose the minimizing of the Root Mean Square (RMS) variation of the cumulative distribution function in order to obtain a smooth distribution. This sampling resulted in a factor matrix $\mathbf{X}$ of $n = 6$ columns and $m = 100$ rows with an average shortest distance between points of 0.72 ± 0.23.

2.2.3 Responses

Two different responses were studied: the stabilizing effect of the brace along the P-A movement and the pressures on the skin. The relevance of these indexes will be discussed in Section 4.1.3. Calculations were performed with Matlab®.

2.2.3.1 Joint stiffening. The response of the limb only was computed thanks to a simulation without bracing and subtracted from the braced limb responses in order to get rid of the skin stiffness contribution. A typical response of the reaction force of the tibia along the P-A direction as a function of the applied P-A drawer magnitude is depicted in Figure 5. The analysis yielded minor damping effects due to the Explicit solver. These oscillations were filtered by a quadratic regression. In all cases, responses were nicely fitted by this kind of polynomial. Finally, the sagittal-plane shear stiffness of the orthosis was calculated as the slope of the 2nd order polynomial at a displacement of 5 mm (see Figure 5). Eagar et al. (2001) showed that the typical load-displacement curve of a knee exhibits a low stiffness region followed by a high stiffness region. This transition appeared at a displacement of $\sim$5 mm and is caused by the tension of passive structures, especially the ACL. The k index is related to this behaviour. This index was calculated for the 100 simulations resulting in a response vector $\boldsymbol{k} = \{k_1, k_2, ..., k_{100}\}$.

2.2.3.2 Pressure distribution. The pressure field applied by the brace on the skin elements was extracted and the mean pressure was computed. This discomfort tolerance index was calculated for the 100 simulations resulting in a response

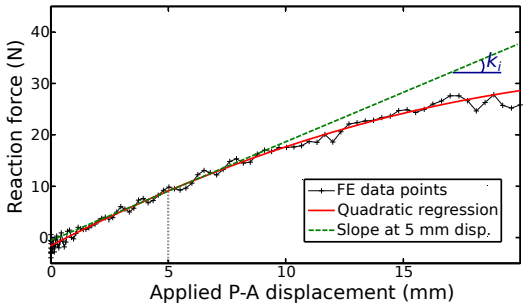

Figure 5. Reaction force of the tibia along the P-A direction vs. applied P-A drawer magnitude to determine k.

vector $\boldsymbol{p} = \{p_1, p_2, ..., p_{100}\}$. Although the pressure field was not uniform, the mean pressure was chosen over the maximum pressure because a global index was judged more reliable than local maxima, which might be influenced by element size and numerical singularities.

2.2.4 Response surfaces

6-dimensional response surfaces f and g respectively express stiffness and discomfort tolerance indexes $\boldsymbol{k}$ and $\boldsymbol{p}$ as a function of the factor matrix $\mathbf{X}$:

$$\begin{aligned} \boldsymbol{k} &= f(\mathbf{X}) + \boldsymbol{\epsilon}_{\mathbf{k}} \\ \boldsymbol{p} &= g(\mathbf{X}) + \boldsymbol{\epsilon}_{\mathbf{p}} \end{aligned} \tag{5}$$

$\boldsymbol{\epsilon}_k$ and $\boldsymbol{\epsilon}_p$ are the residuals due to the lack of fit, depending on the fitting accuracy of chosen functions f and g.

Different functions f and g were fitted on the simulated data. A first degree polynomial response (6 linear coefficients + 1 constant term) was primarily fitted with a multi-dimensional linear regression method. Each polynomial coefficient is the partial derivative of the response with respect to a factor, thus it represents the global influence of this factor on the studied response. Then a second degree polynomial response with full interactions (6 linear coefficients + 21 quadratic coefficients + 1 constant term) was fitted to study the level of interactions between factors. Finally, an interpolation was performed thanks to a sum of radial basis functions (RBFs), as described in Matlab (2011). This function matches values of all data points and interpolates between them, hence residuals are equal to zero. A multiquadratic base was used. The obtained fit functions f_{rbf} and g_{rbf} were used to perform a parameter optimization.

Different statistical methods were used to assess the fitting accuracy. The Root Mean Squared Error (RMSE) and the Predicted Residual Sum of Squares Root Mean Square Prediction Error (PRESS RMSE) were calculated for the linear and quadratic regressions. A Fisher's test was applied on the quantity defined as the ratio of Mean Square of Regression (MSR) to Mean Square Error (MSE) in order to test the overall model significance. A Student's test was applied to each coefficients in the model to test their individual significance.

2.2.5 Design optimization

Thanks to both index response surfaces interpolated with RBFs, it is possible to compute a brace design for which parameters would be optimised to maximize the stiffness index while minimizing the discomfort tolerance index. With this in mind, a tolerance threshold was set to various values to investigate the optimal brace design corresponding to a discomfort tolerance level. A genetic algorithm (Matlab 2011) was used in Matlab® with enough runs to ensure a global minimization. The

Table 3. Characteristics of simulations A and B.

	Simulation A	Simulation B
k index value (N/mm)	10.9	0.58
p index value (kPa)	23.5	0.79
Soft tissue stiffness (kPa)	400	5
Brace circumference (cm)	30.1	37.7
Brace height (cm)	17	51
Fabric stiffness (kN/m)	2.00	0.96
Friction coefficient (-)	0.26	0.84
Initial strap strain (%)	14	5

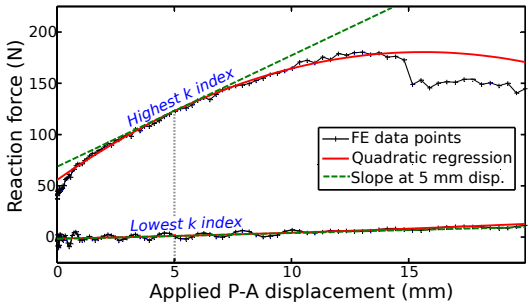

Figure 6. Reaction force of the tibia along the P-A direction vs. applied P-A drawer: joint stabilizing effect of simulations A and B (maximum and minimum stiffness indexes). The response of the limb only has been subtracted.

fitness function to maximize was set to f_{rbf} and a non-linear constraint function was chosen such as $g_{\text{rbf}} \leq p_t$ with p_t a given mean pressure tolerance threshold.

3. Results

3.1 Exploratory FE results

A single FE analysis completed in about 6 hours on 8 CPUs at 2.4 Ghz. All 100 simulations were completed successfully. The mechanical equilibrium was checked by observing energy quantities to verify that dynamic effects had dampened out. Because of the various factor values that were simulated, no general results can be given. Instead two extreme cases were selected: simulations A and B yield the highest and lowest stiffness indexes respectively. The characteristics of these simulations are reported in Table 3.

3.1.1 Reaction forces

The response curves of both these simulations are reported in Figure 6. Not only did simulation A exhibit a higher stiffness index, it also had a high reaction force at zero displacement. This means that this brace alters the natural resting position of the joint. This behaviour was observed for some high k index simulations. What is more, a reaction force drop can be noticed at 15 mm for this brace. A deeper analysis of the results showed a stick-and-slip behaviour: a mechanical discontinuity (balance between normal and tangential forces) suddenly allowed the brace to slip where it previously adhered to the skin, leading to a sudden mechanical efficiency loss.

3.1.2 Strains

Strain results in the fabric are reported in Table 4. For simulation A, the fabric strain was quite high in the circumferential direction after the fitting step due to the small initial circumference of the brace. However the fabric deformed mainly in the

Table 4. Fabric strain results for simulations A and B.

Sim.	Direction	Strain (%) at the end of fitting step: mean (min/max)	Strain (%) at the end of drawer step: mean (min/max)
A	Long.	0.13 (-12/20)	3.9 (-21/29)
	Circ.	22 (7.8/39)	24 (6.6/39)
	Shear	-0.39 (-17/11)	-0.33 (-21/14)
B	Long.	0.35 (-2.7/8.8)	0.4 (-5.6/8.6)
	Circ.	2.2 (3.9/11)	2.4 (-3.8/14.8)
	Shear	-0.13 (-7.4/7.3)	-0.15 (-8.8/9.1)

longitudinal direction during the drawer step. Some creases appeared on the brace fabric in the popliteal area (behind the joint) for simulation B due to the buckling of shell elements under compressive forces. These creases are usually observed on real braces in this region. A higher compression of soft tissues observable on real braces at the brace/limb interfaces and under the straps was also observed in these FE results. Skin did not deform much during the fitting step: compressive logarithmic strains of 20–30 % were located underneath the brace for simulation A and 10–20 % in the patella area for simulation B.

3.1.3 Contact pressure

A very inhomogeneous pressure distribution was observed for both simulations, as depicted in Figure 7. Concerning simulation A, very high local pressures were located underneath the straps and the rigid bars. Such high values (mean pressure of 23.5 kPa and local values up to 398 kPa) would probably lead to serious discomfort. This is why the brace from simulation A, although very efficient for preventing a drawer, is not an acceptable design. Here lies the interest of the parametric study and the optimization of a effective brace design which does not apply too high pressure. Simulation B exhibited lower pressures. Maximum local pressures were located on the patella, the tibia area and below the rigid bars, but their magnitudes were considerably lower than simulation A (mean pressure of 0.79 kPa and local values up to 8.61 kPa). Large areas were even not in contact with the brace due to its low tightening.

3.1.4 Interface sliding

The skin/soft tissues interface exhibited substantial sliding in our simulations. Sliding magnitudes after the drawer step reached about 1.5 cm all around the thigh and leg under the braced area for tight, short braces on contracted limbs. The brace also moved relative to the skin for such braces with a magnitude of $\sim$2 cm in the same area, but this sliding was much more localized in the popliteal area within the thigh/leg interface area and the brace adhered everywhere else.

3.2 Design of experiments and optimization results

The mean ($\pm$ st. dev.) k value for all the simulations was 3.18 ($\pm$ 2.22) N/mm. Maximum and minimum values were 10.9 and 0.58 N/mm. p values averaged 6.63 ($\pm$ 4.45) kPa with maximum and minimum values of 23.5 and 0.72 kPa. In all cases, the overall model significance was higher than 0.9999.

3.2.1 Linear regression

The linear regression with 7 terms exhibited a RMSE of 1.25 N/mm and a PRESS RMSE of 1.31 N/mm for the stiffness index, a RMSE of 2.09 kPa and a PRESS RMSE of 2.20 kPa for the discomfort tolerance index.

The computed polynomial coefficients for both responses are represented in Figure 8. Each coefficient is representative of the influence of a factor on the overall

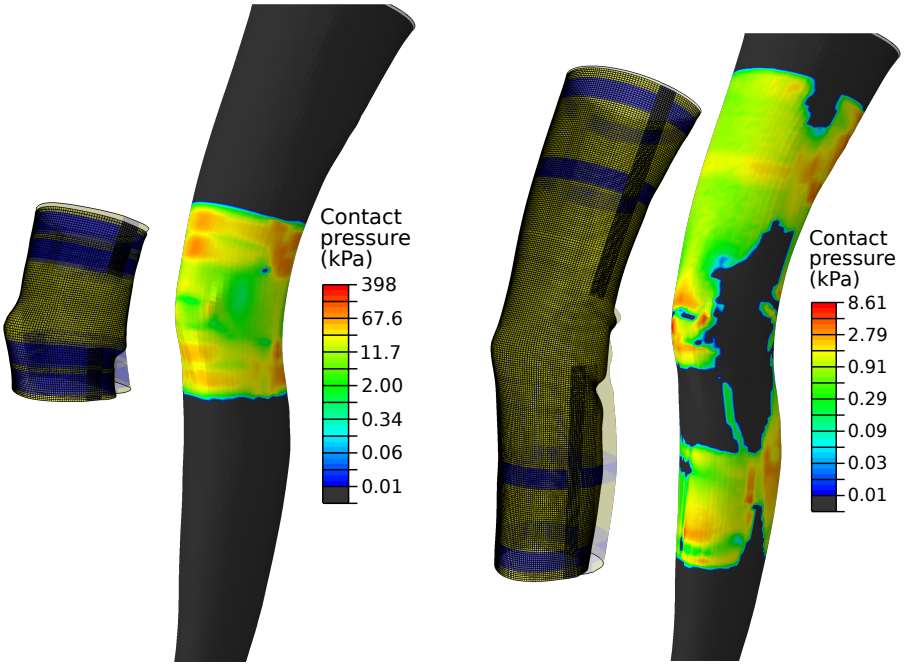

(a) Simulation *A*. *(b)* Simulation *B*.

Figure 7. Deformed brace mesh after the drawer step (shape before drawer in overlay) and pressure map on the surface of the skin for both simulations (log. scale).

response. For example, by increasing the fabric stiffness of 1 in the coded space (*i.e.* 0.75 N/m), the brace reaction to a drawer is expected to increase of 950 N/mm and the mean pressure of 1.91 kPa. Surprisingly, the brace length was found to be the most influential factor for joint stiffening, and in favour of the small brace. The most influential parameter for the p-response was the strap tightening. The friction coefficient had a relatively low influence on both responses. Comparing the influence of each coefficient on both responses, it was found that increasing the k-index of 1 N/mm lead to an increase of the p-index of about 2 kPa. This finding is valid when changing the soft tissue stiffness, the brace size and the fabric stiffness. Increasing the friction coefficient allowed to increase the k-index without significantly increasing the mean pressure, but only to a small extent. However, the brace length and strap tightening were found to be key parameters because they gave strong leverage on an index but not much on the other.

3.2.2 Quadratic regression

Concerning the quadratic regression, the terms which turned out to be insignificant ($p<0.95$) were removed. For the stiffness index, 15 terms were retained. The regression had a RMSE of 0.58 N/mm and a PRESS RMSE of 0.64 N/mm. For the discomfort tolerance index, 20 terms were retained, resulting in a RMSE of 0.59 kPa and a PRESS RMSE of 0.70 kPa. The computed coefficients are represented in Figure 9. Colour intensities show the influence of each term, therefore the interaction levels between parameters can be easily visualized. This revealed that some terms interact strongly. For the k-response, soft tissue stiffness with brace length and strap tightening with brace length had the higher interaction coefficients. The quadratic term associated with brace length was also high, indicating a strongly non-linear response. For the p-response, soft tissue stiffness with strap tightening and strap tightening with brace length had the higher interaction coefficients.

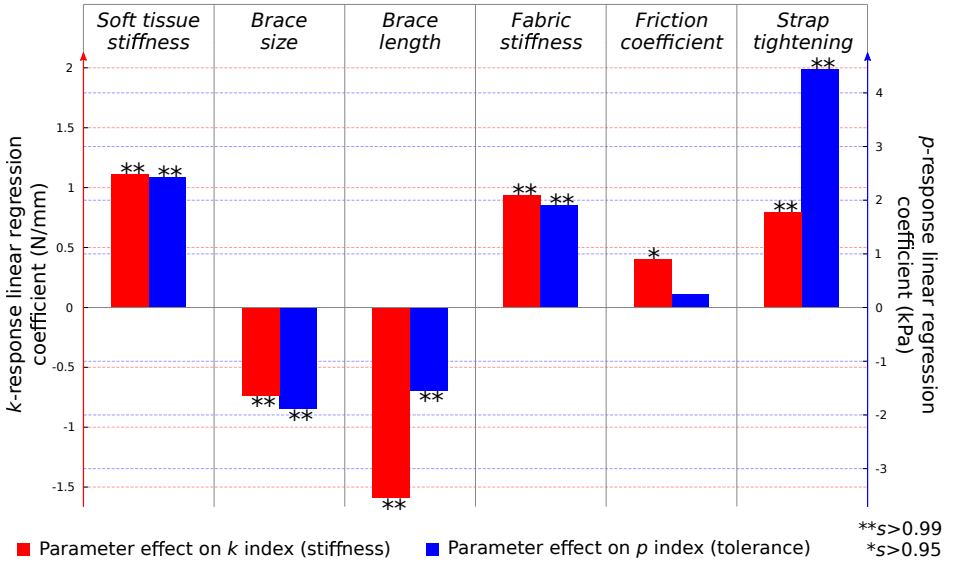

Figure 8. Coefficient values for the linear regression on both responses in the coded space. s stands for significance.

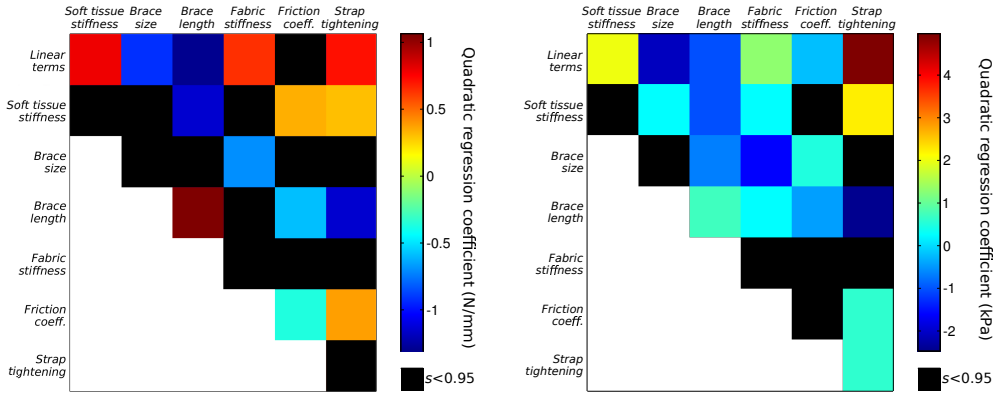

(a) k response. *(b)* p response.

Figure 9. Coefficient values for the quadratic regression on both responses in the coded space (graphic representation of the interaction matrices). s stands for significance.

3.2.3 Brace optimization

The exploitation of these results naturally leads to an optimization of the brace design in order to maximize the k index without exceeding a certain pressure threshold. As the soft tissue stiffness is a patient-related parameter, the design was separated between two half-planes, resulting in two responses for each index: first an optimised brace for a passive limb, then an optimised brace for a contracted limb. Finally, it was hypothesized that a compromise could be reached for a brace that applies low pressures during muscle rest and a maximized joint stabilization during muscle contraction, for instance during the stance phase of gait. The results of these optimizations are reported in Table 5.

It is noteworthy that the indicated brace size (33 cm) for this limb in the manufacturer's size table was found to be close to optimal values. Fabric stiffness was found to be a parameter that should be maximized. Finally, strap tightening appeared to be a very efficient parameter to navigate between different pressure thresholds.

Table 5. Characteristics of optimised braces.

	Passive limb			Active limb			Compromise		
Passive p value (kPa)	3*	4*	5*	-	-	-	3*	4*	5*
Passive k value (N/mm)	2.83**	3.21**	3.54**	-	-	-	2.79	3.17	3.49
Active p value (kPa)	-	-	-	3*	4*	5*	8.34	9.53	10.59
Active k value (N/mm)	-	-	-	6.42**	6.90**	7.41**	6.82**	9.22**	11.65**
Brace circumference (cm)	32.9	31.9	31.1	33.5	34.0	33.8	33.7	32.7	31.9
Brace height (cm)	17	17	17	17	17	17	17	17	17
Fabric stiffness (kN/m)	1.98	1.96	1.96	2	2	2	2	2	2
Friction coefficient (-)	0.48	0.45	0.42	0.93	0.76	0.70	0.60	0.58	0.56
Initial strap strain (%)	7.5	8.5	9.4	5.5	6.3	6.9	7.9	8.9	9.9

*Threshold not to be exceeded.

**Maximized index.

4. Discussion

4.1 Methodological justifications

4.1.1 Finite element model

The proposed finite element model of the deformable limb is not patient-specific, it is a generic model representative of a median male lower limb. Some studies in the literature highlight the importance of patient-specific geometry and mechanical properties for biomechanical studies. For example, Dubuis (2011) showed a significant inter-subject variability of pressure levels applied by elastic compression. Even if it has not been demonstrated, it is highly probable that several patient-specific factors influence the mechanical response of the brace-limb system such as mechanical properties of the different limb constituents (skin, soft tissues) as well as the thickness of adipose tissue or the geometry of the limb itself. The same remark is valid for the finite element brace. It is mechanically representative of usual commercially available braces but some specificities are missing. For instance, most braces have a patella opening with a silicon ring. In view of simplification, this feature was not implemented in this model. It is designed to enhance the flexural behaviour of the brace during knee bending. It requires further investigation to confirm that a patella opening has a limited mechanical effect on both indexes. Nevertheless, the purpose of this work is not to compute the actual response of a particular brace-limb system, but to understand the general mechanisms governing force transfers. In that way, the developed generic model is representative of a median limb with a general brace and is perfectly suited for exploratory biomechanical investigation.

Concerning the interfaces, the model allows skin sliding on underlying tissues and brace sliding on skin. The latter phenomenon leads to brace migration, it is problematic for patients and well known in clinical practice (rehabilitation and sport). Industrials have tried to limit this sliding by attaching adhesive silicon pads at some places inside the brace. These pads were not modelled as such, but changing the global orthosis/skin friction coefficient accounted for this feature. This study shows that they have a limited impact on both responses, but still it appeared that it allowed to gain little efficiency without altering the mean pressure (Figure 8). However these pads are essentially meant to prevent sliding during knee bending and in dynamic conditions (Van Leerdam 2006). As for the skin/soft tissues interface, it must be emphasized that there is a strong lack of mechanical data in the literature. This interface would probably exhibit a more complex behaviour than a basic isotropic quasi-frictionless Coulomb friction model, but our model is a good approximation for low sliding magnitudes, which is the case in most areas.

It was chosen not to model the intra-articular joint elements (cartilage, liga-

ments...) because this would be computationally expensive and the goal was to study the effect of braces on the joint stiffening and not on inner structures. This is why a simple translation was applied as a BC to approximate the motion of a real ACL-deficient joint instability. This kinematics may also be subject to discussion. Christel et al. (2012) investigated the actual kinematics during an anterior translation caused by the Lachman test; they showed that a complete removal of the ACL resulted in almost pure tibial translation. Lujan et al. (2007) suggested that the ACL encourages internal rotation by "unwinding" during anterior translation. The choice of constraining the DOFs and allowing only anterior tibial translation was made to reproduce a injured kinematics; it will thus be possible to compare previous and future results with this study, as it is a standard test in the medical field to assess knee stability after an ACL rupture (cadaveric studies, Lachman test, arthrometers such as the KT-1000, etc...). What is more, it has the advantage of being numerically much more stable.

Finally, another strong assumption of the model is the quasi-static analysis. Knee instabilities are often characterized by a rapid motion of one segment with respect to the other. The dynamic response of the brace-limb system may be slightly different from the quasi-static response. The textile used for braces often includes a high ratio of synthetic fibres, which exhibit a viscoelatic behaviour, as do body tissues. However, the factor domains cover the eventual stiffness increase of materials for rapid solicitation. Dynamic forces induced by acceleration have almost no effect on the brace because of its low mass. The quasi-static approach is then an appropriate approximation.

4.1.2 Design of experiment

The method of design of experiment is a solid approach to investigate the influence of each factor, however the results are dependent of the choice to include or not a factor, and of the chosen domains. The number of investigated factors was first dictated by the maximum number of simulations that could be performed in a reasonable amount of time. Several factors were omitted either in a concern of simplification (influence of a patella opening, of brace misalignment, of fabric anisotropy and of patient specific factors) or because they were thought to have low mechanical impact on the studied responses (effect of helical straps, strap stiffness, and of the articulation system linking bars).

All these factors proved to interact strongly for both responses, as seen in Figure 9. This means that the linear regression is only a rough approximation of the responses, as shown by the RMSEs. However it is easy to interpret, as each coefficient value is the overall effect of the corresponding factor. The quadratic regression is a highly accurate response, the RMSEs are relatively low. As some parameters are aliased, it is more complicated to physically explain each polynomial factor. Concerning the interpolation by radial basis functions, it passes through all test points so the RMSE is zero. But this does not mean that it would predict the responses of a new simulation without error, because the distance between test points is quite large compared to the size of the domain. This is especially true at the borders of the domain where the functions are extrapolated. This is why a validation test was performed to predict the response of two optimised braces from Table 5. The first is the brace for a passive limb with a pressure threshold of 4 kPa, with a predicted k value of 3.21 N/mm. A FE analysis of this parameter set yielded a p value of 4.12 kPa and a k value of 3.27 N/mm (errors of 3 and 2 %). The second is the brace for an active limb with a pressure threshold of 4 kPa, with a predicted k value of 6.90 N/mm. The FE analysis of this parameter set computed a p value of 3.97 kPa and a k value of 6.02 N/mm (errors of 1 and 13 %).

4.1.3 Stiffness and discomfort tolerance indexes

Both indexes were chosen as the primary aim of a knee brace: increasing joint stability while being relatively comfortable.

The k index is a good indicator of the additional stiffness brought by the brace at low anterior displacement. This implies the hypothesis that the stiffness response of a braced joint under a drawer is the sum of the inherent joint stiffness with the additional brace stiffness, as the stiffness of two springs in parallel is the sum of each individual stiffness. This index does not account for the initial force, which was not negligible for some braces, as seen in Figure 6 and could help maintaining knee stability by replacing the ACL initial tension, as highlighted by Solomonow (2006).

The idea behind the p index is to quantify discomfort as a global tolerance level. However, discomfort tolerance is a very subjective sensation and depends not only on the mean pressure but also on local cutaneous solicitations (pinching, denting), on the solicited area, fabric type, etc... The literature is very scarce in comfort/tolerance assessment. As orthotic devices are typically worn for a few hours, global discomfort tolerance might be estimated by avoiding pressures above the ischemic level, *i.e.* the level at which capillaries are unable to irrigate tissues. The value of 4.3 kPa from the work of Landis (1930) is traditionally used.

4.2 Result outcomes

The main effects governing brace efficiency and their effect on joint stabilization are described here. Some practical learnings for manufacturers and physicians are also given.

4.2.1 Force transfer mechanisms

Two main force transfer mechanisms have been identified: the sleeve compression effect and the force transmission efficiency from the bars to the straps.

The first effect depends on the pressure applied by the brace on the skin due to elastic compression. The brace stiffening efficiency greatly depends on these compressive forces. In fact, the brace is secured to the limb (no slip) at a point if:

$$F_t \leq \mu \, F_n \tag{6}$$

with F_t and F_n the tangential and normal forces and μ the friction coefficient of the interface. Compressive forces are thus related to the resistive forces preventing the drawer. The Laplace law for elastic compression says that F_n is proportional to the tension in the fabric along the circumferential direction (Dubuis 2011):

$$P = \frac{F_n}{a} = \frac{T}{r} \tag{7}$$

with P the pressure applied by the brace, T the tension in the circumferential direction of the fabric, r the curvature radius in the same direction and a the area. F_n is then maximized by increasing fabric stiffness and decreasing the initial brace circumference. However, it also increases the mean pressure, this explains why these two factors had the same relative effect on k and p (Figure 8). This compression effect also limits skin sliding on soft tissues, but to a lesser extent because of the lower friction coefficient.

The second effect is the efficiency of force transfer from the bars to the straps. It can be explained by considering the attach between straps and rigid bars as

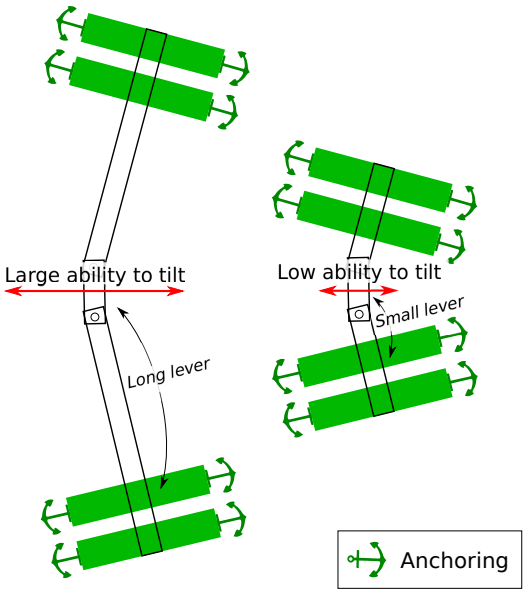

Figure 10. Mechanism explaining the advantage of small braces to prevent drawer.

anchoring points of the brace on the limb, as depicted in Figure 10. The stabilizing effect is affected by the movement of bars relative to the limb segments (loosening). As the strap fabric is much stiffer than the brace fabric, the latter one deforms easily. The ability to tilt the hinge link depends on the strength of anchors and the lever arm, *i.e.* on the strap tightening and the brace length. If the straps are attached to the bars far away from the joint, there is a long lever arm and tilting the hinge link is easy; in contrary, a small lever arm makes it more resistant to tilting. As a matter of fact, the brace length might be misleading, a long brace with anchoring points (straps) close to the joint would probably result in the same improvement. This effect is essential for designing an optimised brace because it allows to increase the force transfer without necessarily increasing the mean pressure, unlike the previous effect. This effect explains the major interaction between strap tightening and brace length for the k index (Section 3.2.2).

4.2.2 Mechanical stiffening level

It has been found that conventional braces have a joint stiffening effect and this effect has been quantified and optimised. Liu et al. (1994) experimentally tested 10 braces on a surrogate leg using the same kinematics. From their data, an average k-index of 11.3 N/mm (min: 5.1, max: 18.3) has been computed. These values are high, and it is probable that the testing support has a high influence because a rigid leg was used, and the stiffening effect may be overestimated. This study proves that the mechanical realism of the testing support is important and the use of FE modelling allowed to obtain more reliable responses.

It is hard to tell if the computed stabilization levels are high enough to efficiently reduce an actual drawer laxity. Eagar et al. (2001) performed the same P-A test on 7 cadaveric knees, with and without the ACL. Results of this study are shown in Figure 11 and clearly illustrate the high laxity of an ACL-deficient knee. The response of a brace with a k index of 8 N/mm has been plotted and added to the ACL-deficient knee in order to predict the response of a braced injured knee: it compensates the injury and is comparable to the healthy knee for low displacements.

However, joint stability also comes from muscle activation. Wojtys et al. (2002) used an arthrometer to measure sagittal-plane shear stiffness of passive and ac-

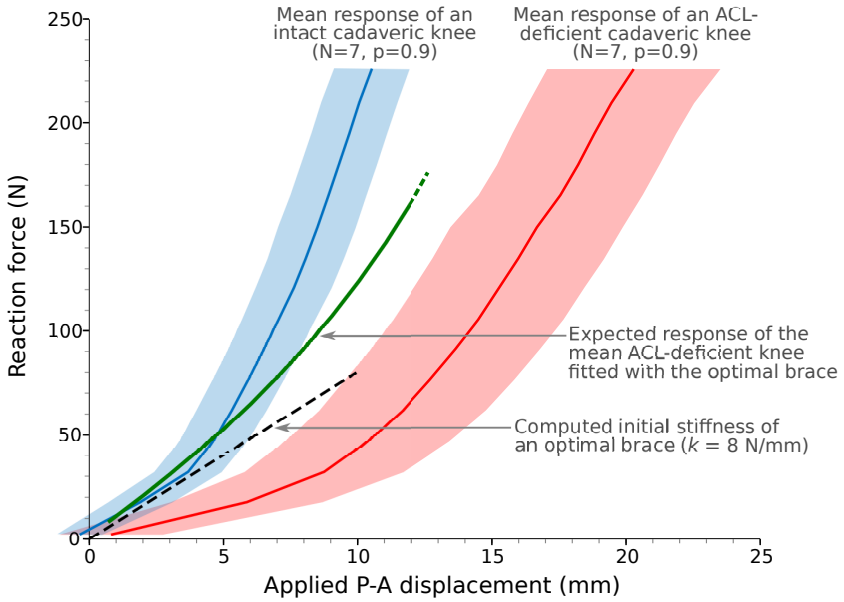

Figure 11. Quantification of the additional stiffness brought by an optimal brace ($k = 8$ N/mm) to an ACL-deficient cadaveric knee under a P-A displacement. Data kindly provided by Eagar et al. (2001).

tive knees. Passive knees exhibited a mean stiffness of 18.7 N/mm (men) and 19.3 N/mm (women) while active limbs resulted in stiffer joints: 70.9 N/mm (men) and 40.7 N/mm (women). A good order of magnitude of *in-vivo* forces in the knee was given by Kutzner et al. (2010), who measured anterior forces as high as 30 % bodyweight (240 N for 80 kg) when descending stairs. The passive structures only need to bear a small fraction of this force when muscles are contracted. That is, the stabilizing effect of an optimised brace could be enough to compensate for a deficient ACL if the muscles are recruited as the main active stabilizers.

The sufficiency of the stiffening effect of the brace remains a difficult question because the ACL is not only a passive stabilizing mechanical structure, but also a major sensory organ capable of stimulating the active recruitment of the musculature to participate in maintaining joint stability (Solomonow 2006). An optimised brace could compensate the mechanical deficiency at low forces/displacements, but it is not sure at which extent it can compensate the lack of sensory feedback by proprioceptive effect. If it turns out that braces can effectively trigger muscle contraction thanks to this effect, the joint stiffening induced by muscle contraction would be much higher that what is brought by the brace. Several studies show that muscle activation is modified by such devices (Osternig and Robertson 1993; Ramsey et al. 2003; Théoret and Lamontagne 2006), but the level of actions are not known and the mechanisms not fully understood.

Finally, in order to restore the ACL function, a brace should not only restrain anterior tibial translation but also restore internal tibial rotation during the drawer (Lujan et al. 2007). The simulated 1-DOF kinematics does not allow the tibia to rotate, but this effect can be investigated by looking at the internal tibial moment during the motion. This moment was found to be very low (-0.1 to 0.3 N.m depending on the case), probably due to the symmetric design of the brace.

4.2.3 Brace design and fitting recommendations

As for now, most investigated design parameters are chosen arbitrarily or empirically. This study suggests a few guidelines to design more efficient and comfortable braces. These braces should be seen as prototypes because they were optimised only for two purposes, which are drawer prevention and discomfort tolerance; they

might not be suitable for unusual limb geometries, high flexion angles... Knowing this, the brace size from the manufacturer's size chart was found to be adapted to this limb. Anti-sliding pads systems are probably more efficient to limit dynamic sliding rather than to improve sagittal-plane shear stiffness. Besides, it is recommended to use stiffer fabric than usually found for the brace body. Further investigations are needed to determine whether a stiffness of 2 kN/m is convenient for knee bending. Finally, the most important recommendation is to attach the straps close to the joint, in order to keep a short lever arm between the centre of the joint and the rigid anchoring points. This can be done by designing shorter braces, which could reduce manufacturing costs. A non-symmetric design (of the body or straps) could help restoring the internal tibial rotation during the drawer.

Practitioners should insist on the fact that a correct strap tightening is very important when prescribing a brace to a patient. If the straps are too loose, they do not play their role of anchoring points effectively. It they are too tight, the applied pressure is too high and the discomfort tolerance is increased.

5. Conclusion

An original FE model of a braced deformable limb has been developed and used to assess the influence of various design factors of usual knee braces on the ability to prevent a drawer. Two efficiency indexes have been proposed: the mechanical stabilization (stiffening) of the joint and the pressure applied onto the skin. A parametric optimization resulted in brace designs yielding a stiffening effect high enough to compensate for the structural role of the ACL at low displacement. Two main force transfer mechanisms have been identified: a sleeve compression effect and a load transfer to the side bars through the straps. The latter is governed by strap tightening and brace length, which were found to be key factors to improve brace designs. This study proposes a new methodology to assess the biomechanical efficiency of knee orthoses and provides substantive guidance to manufacturers and practitioners. The model and findings will be validated in future studies, first through experimental measurements with an instrumented limb simulator, then through a clinical trial using an arthrometer. The characterization of commercially available braces will lead to an objective ranking based on their stiffness index. Finally, the role of orthoses on inner structures (muscles, ligaments) needs to be investigated to understand how other mechanisms such as proprioceptive action, localized structural unloading or muscle recruitment participate in the brace effect.

Acknowledgements

This work was funded in part by the ANRT (Association Nationale de la Recherche et de la Technologie) and the following orthotic manufacturers: Thuasne®, Gibaud® and Lohmann-Rauscher®.

References

Abaqus. *ABAQUS 6.10-2 User Documentation*. Simulia, Dassault Systems. 2010.

Albin TJ. 1987. In Vivo Estimation of the Coefficient of Friction between Extrinsic Flexor Tendons and Surrounding Structures in the Carpal Tunnel. Proceedings of the Human Factors and Ergonomics Society Annual Meeting 31(3):323–324.

Avril S, Bouten L, Dubuis L, Drapier S, Pouget JF. 2010. ASME; Mixed Experimental and Numerical Approach for Characterizing the Biomechanical Response of the Human Leg Under Elastic Compression. Journal of Biomechanical Engineering 132(3), 031006.

Barrack RL, Skinner HB, Buckley SL. 1989. Proprioception in the anterior cruciate deficient knee. The American Journal of Sports Medicine 17(1):1–6.

Beaudreuil J, Bendaya S, Faucher M, Coudeyre E, Ribinik P, Revel M, Rannou F. 2009. Clinical practice guidelines for rest orthosis, knee sleeves, and unloading knee braces in knee osteoarthritis. Joint Bone Spine 76(6):629–636.

Beynnon BD, Fleming BC. 1998. Anterior cruciate ligament strain in-vivo: A review of previous work. Journal of Biomechanics 31(6):519–525.

Beynnon BD, Johnson RJ, Fleming BC, Peura GD, Renstrom PA, Nichols CE, Pope MH. 1997. The Effect of Functional Knee Bracing on the Anterior Cruciate Ligament in the Weightbearing and Nonweightbearing Knee. The American Journal of Sports Medicine 25(3):353–359.

Birmingham TB, Kramer JF, Kirkley A, Inglis JT, Spaulding SJ, Vandervoort AA. 2001. Knee bracing for medial compartment osteoarthritis: effects on proprioception and postural control. Rheumatology 40(3):285–289.

Bollen S. 2000. Epidemiology of knee injuries: diagnosis and triage. British journal of sports medicine 34(3):227–228. PMID: 10854030

Cawley PW, France EP, Paulos LE. 1989. Comparison of rehabilitative knee braces. The American Journal of Sports Medicine 17(2):141 –146.

Christel PS, Akgun U, Yasar T, Karahan M, Demirel B. 2012. The contribution of each anterior cruciate ligament bundle to the Lachman test: a cadaver investigation. The Journal of bone and joint surgery. British volume 94(1):68–74. PMID: 22219250

Corrigan J, Cashman W, Brady M. 1992. Proprioception in the cruciate deficient knee. Journal of Bone and Joint Surgery, British Volume 74-B(2):247–250.

Dubuis L, Avril S, Debayle J, Badel P. 2012. Identification of the material parameters of soft tissues in the compressed leg. Computer Methods in Biomechanics and Biomedical Engineering 15(1):3–11. PMID: 21809938

Dubuis L. 2011. Biomechanics of soft tissues of human leg under elastic compressionEcole Nationale Supérieure des Mines de Saint-Etienne.

Eagar P, Hull ML, Howell SM. 2001. A method for quantifying the anterior load-displacement behavior of the human knee in both the low and high stiffness regions. Journal of Biomechanics 34(12):1655–1660.

Evans SL, Holt CA. 2009. Measuring the mechanical properties of human skin in vivo using digital image correlation and finite element modelling. The Journal of Strain Analysis for Engineering Design 44(5):337–345.

Fleming BC, Renstrom PA, Beynnon BD, Engstrom B, Peura G. 2000. The Influence of Functional Knee Bracing on the Anterior Cruciate Ligament Strain Biomechanics in Weightbearing and Nonweightbearing Knees. The American Journal of Sports Medicine 28(6):815–824.

Flynn C, Taberner A, Nielsen P. 2010. Mechanical characterisation of in vivo human skin using a 3D force-sensitive micro-robot and finite element analysis. Biomechanics and Modeling in Mechanobiology 10(1):27–38.

France EP, Paulos LE. 1990. In vitro assessment of prophylactic knee brace function. Clinics in Sports Medicine 9(4):823–841.

France EP, Paulos LE, Jayaraman G, Rosenberg TD. 1987. The biomechanics of lateral knee bracing. The American Journal of Sports Medicine 15(5):430–438.

Genty M, Jardin C. 2004. Place des orthèses en pathologie ligamentaire du genou. Revue de la littérature. Annales de Réadaptation et de Médecine Physique 47(6):324–333.

Gerhardt L, Lenz A, Spencer ND, Münzer T, Derler S. 2009. Skin-textile friction and skin elasticity in young and aged persons. Skin Research and Technology: Official Journal of International Society for Bioengineering and the Skin (ISBS) and International Society for Digital Imaging of Skin (ISDIS) and International Society for Skin Imaging (ISSI) 15(3):288–298. PMID: 19624425

Gordon MD, Steiner ME. 2004. Anterior cruciate ligament injuries. Orthopaedic Knowledge Update: Sports Medicine. Rosemont, IL: American Academy of Orthopaedic Surgeons pp. 169–181.

Goupy J, Creighton L. 2007. Introduction to Design of Experiments with JMP Examples, Third Edition. 3 ed. SAS Institute.

Guimberteau J, Sentucq-Rigall J, Panconi B, Boileau R, Mouton P, Bakhach J. 2005. Introduction à la connaissance du glissement des structures sous-cutanées humaines. Annales de Chirurgie Plastique Esthétique 50(1):19–34.

Hinterwimmer S, Graichen H, Baumgart R, Plitz W. 2004. Influence of a mono-centric knee brace on the tension of the collateral ligaments in knee joints after sectioning of the anterior cruciate ligament - an in vitro study. Clinical Biomechanics 19(7):719–725.

Iivarinen JT, Korhonen RK, Julkunen P, Jurvelin JS. 2011. Experimental and computational analysis of soft tissue stiffness in forearm using a manual indentation device. Medical Engineering & Physics 33(10):1245–1253.

Institut Français du Textile et de l'Habillement. 2006. Campagne Nationale de Mensuration .

Kutzner I, Heinlein B, Graichen F, Bender A, Rohlmann A, Halder A, Beier A, Bergmann G. 2010. Loading of the knee joint during activities of daily living measured in vivo in five subjects. Journal of Biomechanics 43(11):2164–2173.

Landis EM. 1930. Micro-injection studies of capillary blood pressure in human skin. Heart 15(May):209.

Linder-Ganz E, Shabshin N, Itzchak Y, Gefen A. 2007. Assessment of mechanical conditions in subdermal tissues during sitting: a combined experimental-MRI and finite element approach. Journal of Biomechanics 40(7):1443–1454.

Liu SH, Lunsford T, Gude S, , C TVangsness J. 1994. Comparison of functional knee braces for control of anterior tibial displacement. Clinical orthopaedics and related research (303):203–210. PMID: 8194235

Lujan TJ, Dalton MS, Thompson BM, Ellis BJ, Weiss JA. 2007. Effect of ACL deficiency on MCL strains and joint kinematics. Journal of biomechanical engineering 129(3):386–392. PMID: 17536905

Lunsford TR, Lunsford BR, Greenfield J, Ross SE. 1990. Response of eight knee orthoses to valgus, varus and axial rotation loads. Journal of Prosthetics and Orthotics 2(4):274.

Matlab. *MATLAB R2011a Product Help, MathWorks*. 2011.

McKay M, Beckman R, Conover W. 1979. Comparison of three methods for selecting values of input variables in the analysis of output from a computer code. Technometrics 21(2):239–245.

McNair PJ, Stanley SN, Strauss GR. 1996. Knee Bracing: Effects on Proprioception. Archives of Physical Medicine and Rehabilitation 77(3):287–289.

Melanix. 2012. DICOM sample image sets. http://pubimage.hcuge.ch:8080.

Miyasaka KC, Daniel DM, Stone ML, Hirshman P. 1991. The incidence of knee ligament injuries in the general population. American Journal of Knee Surgery 4(1):43–48.

Olsson A, Sandberg G, Dahlblom O. 2003. On Latin hypercube sampling for structural reliability analysis. Structural Safety 25(1):47–68.

Osternig LR, Robertson RN. 1993. Effects of prophylactic knee bracing on lower extremity joint position and muscle activation during running. The American Journal of Sports Medicine 21(5):733–737.

Paluska SA, McKeag DB. 2000. Knee braces: current evidence and clinical recommendations for their use. American Family Physician 61(2):411–418, 423–424.

Paulos LE, France EP, Rosenberg TD, Jayaraman G, Abbott PJ, Jaen J. 1987. The biomechanics of lateral knee bracing. The American Journal of Sports Medicine 15(5):419–429.

Ramsey DK, Wretenberg PF, Lamontagne M, Németh G. 2003. Electromyographic and biomechanic analysis of anterior cruciate ligament deficiency and functional knee bracing. Clinical Biomechanics 18(1):28–34.

Rasband W. 1997-2011. ImageJ. National Institutes of Health, Bethesda, Maryland, USA .

Ribinik P, Genty M, Calmels P. 2010. Evaluation des orthèses de genou et de cheville en pathologie de l'appareil locomoteur. Avis d'experts. Journal de Traumatologie du Sport 27(3):121–127.

Sanders JE, Greve JM, Mitchell SB, Zachariah SG. 1998. Material properties of commonly-used interface materials and their static coefficients of friction with skin and socks. Journal of Rehabilitation Research and Development 35(2):161–176.

Solomonow M. 2006. Sensory - Motor control of ligaments and associated neuromuscular disorders. Journal of Electromyography and Kinesiology 16(6):549–567.

Thijs Y, Vingerhoets G, Pattyn E, Rombaut L, Witvrouw E. 2009. Does bracing influence brain activity during knee movement: an fMRI study. Knee Surgery, Sports Traumatology, Arthroscopy 18(8):1145–1149.

Thoumie P, Sautreuil P, Mevellec E. 2001. Orthèses de genou. Première partie : Evaluation des propriétés physiologiques à partir d'une revue de la littérature. Annales de Réadaptation et de Médecine Physique 44(9):567–580.

Thoumie P, Sautreuil P, Mevellec E. 2002. Orthèses de genou. Evaluation de l'efficacité clinique à partir d'une revue de la littérature. Annales de Réadaptation et de Médecine Physique 45(1):1–11.

Théoret D, Lamontagne M. 2006. Study on three-dimensional kinematics and electromyography of ACL deficient knee participants wearing a functional knee brace during running. Knee Surgery, Sports Traumatology, Arthroscopy 14(6):555–563.

Tseng Q. 2011. Etude d'architecture multicellulaire avec le microenvironnement contrôlé. Université de Grenoble .

Van Leerdam N. 2006. Chicago, IL: The Genux, A New Knee Brace with an Innovative Non-Slip System. Academy of American Orthotists and Prosthetists .

Vergis A, Hindriks M, Gillquist J. 1997. Sagittal plane translations of the knee in anterior cruciate deficient subjects and controls. Medicine and science in sports and exercise 29(12):1561–1566. PMID: 9432087

Wojtys EM, Ashton-Miller JA, Huston LJ. 2002. Edward M. Wojtys. The Journal of Bone & Joint Surgery 84(1):10–16.

Woo SLY, Fox RJ, Sakane M, Livesay GA, Rudy TW, Fu FH. 1998. Biomechanics of the ACL: Measurements of in situ force in the ACL and knee kinematics. The Knee 5(4):267–288.

Wu Z, Au C, Yuen M. 2003. Mechanical properties of fabric materials for draping simulation. International Journal of Clothing Science and Technology 15(1):56–68.

Yu WR, Kang TJ, Chung K. 2000. Drape Simulation of Woven Fabrics by Using Explicit Dynamic Analysis. Journal of the Textile Institute 91(2):285–301.